THE DEBASEMENT OF THE ROMAN COINAGE IN THE 3RD CENTURY

By Samuel Brew

A project submitted for the Special Academic Extension Course of Sydney Grammar School

June 2021

Abstract

The third century AD was a period of great instability in the Roman Empire, particularly involving the debasement of the coinage from nearly pure silver to mostly bronze. This study aimed to date six Roman *antoniniani* from the third century and link them to this broader trend by using typological analysis to estimate date and XRF and Raman spectrometry, as well as XRF mapping technology, to analyse the compositions of each coin. It was expected that the generally accepted trend of debasement would be proven, and it indeed was, showing that the coinage was indeed debased at an extraordinary rate over the third century, resulting in impure and low-quality currency that led to rampant inflation and contributed to the demise of the Western Roman empire. This analysis also shed light on the concentrations of lead and tin in *antoniniani*, a largely unexplored inquiry, showing the change in the concentrations of metals beyond just silver and copper. By understanding these trends in the compositions of third century Roman coins, we can better understand the nature of the economic crisis which Rome underwent in the period, allowing a greater understanding of some of the factors that led to its collapse.

Acknowledgments

I would like to sincerely thank the following people for their help with this project:

- Dr. Sheridan of Sydney Grammar School for her organisation of this project and expert assistance on the scientific aspects of the project
- Dr. Dearn of Sydney Grammar School for his organisation of this project and expert assistance on the archaeological aspects of the project and in identifying features of the coins themselves
- Dr. Kelloway of Sydney University for her assistance in the operation of the XRF spectrometer and with data interpretation and analysis
- Dr. Ahmed of Sydney University for his assistance in the operation of the Raman spectrometers
- Dr. Stevens of Sydney Grammar School for his organisation and support of the SAC
- Dr. Malpass of Sydney Grammar School for his support of the SAC
- John Story, my colleague in the SAC, for his generous processing of XRF mapping data

Contents

1 Introduction

1.1 Description of Artefacts

The Roman *antoninianus* is the modern numismatist's name for the coin used in the Roman empire after around 214 AD, with the declared value of two *denarii*. Despite this, it was introduced with the weight of just 1.5 *denarii*, meaning its intrinsic value was less than its assumed face value (Metcalf 2012). Over the course of the third century AD, continuing policies of currency debasement in the empire led to a significant reduction in its silver purity, resulting in rampant inflation and contributing eventually to the destruction of the Western Roman empire (Desjardins 2016).

The six *antoniniani* whose analysis will be detailed in this report are of two observable kinds: three appear silvery, and three darker and more copper-like.

As the provenance of these coins was not known, they were referenced throughout the project numerically as coins 1-6. These identifiers do not correspond to date, as they were set before typological analyses had been done, though they are organised such that coins 1-3 appear darker and more copper-like, while coins 4-6 appear more silvery. It should be noted that all coins were in a reasonable condition, all having mostly legible inscriptions on their obverse and reverse, and all with discernible images on both sides.

1.2 Aims and Hypothesis

This report will aim to perform a metallurgical comparison of these six coins, particularly focusing on how the concentrations of different metals changed over time in the Roman *antoninianus*. It will investigate the actual silver concentration of each coin, and determine if a correlation can be made between silver content and the date of an *antoninianus*. If the debasement of the coinage was so pronounced as existing research indicates (Pense 1992) among this small sample, then this should indeed be the case, and silver content should decrease over time, while the concentration of less valuable metals such as copper and tin should increase accordingly. Further, this report will investigate if a correlation can be reasonably drawn between the appearance of a coin as 'silvery' and its actual silver content, which would seem to logically follow. More specifically to the samples, this report will aim to place these coins typologically, and thus identify their date and place of origin.

This analysis utilised primarily XRF spectrometry due to its efficacy for usage in determining the composition of coins (Gentile n.d.), though Raman spectrometry was also used on two of the coins, and the efficacy of this method for determining information about coins broadly, versus XRF, will also be explored.

XRF mapping (two-dimensional XRF spectrometry) was additionally available for the obverse of coin 5, which allows the analysis of how the surface of that coin changes spatially. While interesting, this is unlikely to show any extra information regarding concentration of different metals in the broader picture of the third century AD crisis, and is mostly beyond the scope of this project.

1.3 Roman Debasement of Coinage

The third century AD was a period of great economic upheaval in the Roman empire, as it involved the severe debasement of the currency, inducing economic paralysis and eventually contributing the the collapse of the Western Roman empire by 476 AD (Desjardins 2016). During this period, there were estimated to be around 50 emperors in 50 years, resulting in the need to mint new coins for every single one, as Roman coins were minted with the head of the emperor on the obverse side. AS the Roman currency was based on the *denarius*, a coin with (originally) around 4.5g of pure silver (Desjardins 2016), this mass minting required significant quantities of silver to be available to the empire, which was not the case. In fact, due to the slowing of expansion efforts and the recent exhaustion of major deposits like the Iberian silver mines, the empire's supply of this essential metal was running low.

In an effort to circumvent these issues, Roman emperors attempted multiple methods of debasing the currency – decreasing the intrinsic 'actual' value of coins without decreasing their assumed face value. For example, under Caracalla, the 'double denarius' was issued, which has been named by modern numismatists as the *antoninianus*. This coin was issued to have twice the value of the denarius, however it was in fact only 1.5 times the weight (Metcalf 2012), meaning more coins could be put into circulation without depleting silver resources so much, allowing the emperor to continue his spending, for example to pay his soldiers. Throughout the third century AD, similar practices continued under many emperors, culminating in coins under Gallienus (253-268 ("Gallienus Roman Emperor" n.d.)) having less than 5% silver content (Desjardins 2016). Originally, under Augustus, the denarius had 95-98% silver purity, though over the following 270 years, it came to have around 2%, its final incarnation being a low-quality copper coin with a silver surface. By 280 AD, silver coins had almost entirely lost their value in the empire, which led to Diocletian's reforms in the 4th century AD (Pense 1992).

Once this was discovered early on by the population, many began to hoard the earlier, purer coins, and spend the later, less pure coins. This resulted in rampant inflation, and prices skyrocketed to account for the lower quality currency (Desjardins 2016).

2 Method

2.1 XRF Scanning

Using a Bruker Tracer 5i XRF Spectrometer, I was able to arrive at a series of twelve XRF spectra, one for each side of all six coins. During the process, gloves were worn to prevent damage to the coins, and a radiation shield was placed over the emitting end of the spectrometer.

After the device had been graciously set up by Dr. Kelloway, the following steps were used:

1. Open a new scan on the computer attached to the device.

2. Remove the radiation shield from the device and place the coin in the marked area, with the side to be scanned facing down.
3. Replace the radiation shield over the emitting end of the device, aligning the arrows.
4. Begin the scanning process on the attached computer.
5. Press the trigger on the spectrometer itself (Dr. Kelloway did this due to her credentials).
6. Wait for 30 seconds and then release the trigger.
7. Stop the scanning process on the computer.
8. Save the file as the ID of the scan (e.g. BREW-X-1-O -> Brew XRF Coin 1 Obverse).
9. Repeat steps 1-8 for each scan to be performed.

2.2 Raman Scanning

Using a Bruker BRAVO Handheld Raman Spectrometer, I was able to arrive at a series of four Raman spectra, one for each side of two coins. During the process, laser protection goggles were worn to protect the eyes, and gloves were used to prevent damage to the coins.

After the device had been graciously set up by Dr. Ahmed, the following steps were used:

1. Open the new scan dialogue on the device and enter the ID for the scan (e.g. BREW-R-3-R -> Brew Raman Coin 3 Reverse).
2. Place the coin on the flat surface of a table, with the side to be scanned facing up.
3. Place the probe of the spectrometer on top of the coin, centring the device roughly.
4. Press the scan button and hold the device steadily over the coin until the scan has completed.
5. Repeat steps 1-4 for each scan to be performed.

These scans were then exported from the device and transmitted to me by the university. I was then able to plot the spectra from the given dataset and identify the major peaks.

2.3 XRF Mapping

The coin to be mapped, coin 5, was sent to the university, who performed the process on my behalf using a Bruker ARTAX800 µ-XRF Spectrometer.

3 Results and Discussion

3.1 Typological Placement

Through typological research, particularly using a list of searchable digital references to *The Roman Imperial Coinage* (https://wildwinds.com) and a full database of information about every entry thereof (http://numismatics.org/ocre), I was able to arrive at a reasonable typological placement for each of the six coins, which in turn allowed me to determine their estimated dates and the mints in which they were made.

The table of basic details is provided here for convenience. Note that this also contains the weights of the coins, though those data did not prove useful given the XRF concentration data.

Coin	Date	Weight (g)	Emperor	Mint	RIC Reference
1	293	4.294	Maximian	Cyzicus	RIC V Diocletian 607
2	294	3.872	Diocletian	Antioch	RIC V Diocletian 322
3	272	3.554	Aurelian	Cyzicus	RIC V Aurelian 356
4	239	4.849	Gordian III	Antioch	RIC IV Gordian III 177A
5	247	4.095	Otacilia Severa	Roma	RIC IV Philip I 125C
6	250	4.062	Decius	Roma	RIC IV Trajan Decius 21B

From the aforementioned method, I was able to identify the above data, nearly all of which was mostly derived from the RIC references found.

The set of coins has two examples of each of three mints: Cyzicus, Antioch, and Roma, and 6 independent portrait figures. It should be noted that Maximian (coin 1) was portrayed under what is typologically referred to as the authority of Diocletian, and Otacilia Severa (coin 5) was portrayed under Philip I's authority. The coins date from 247-294, and are all confirmed as *antoniniani*.

It should be noted that I initially misdated coins 2 and 4 by misreading the given information, and coin 4 also by misidentifying the portrayed figure. I noted and corrected these errors later in the analysis stage, though that did result in an early misidentification of the oldest and youngest coins, which were identified as 3 and 5 (respectively), and later corrected to 2 and 4 (respectively). This resulted in three iterations of concentration data analysis, which are describe din further detail below.

See *Appendix 1 – Coin Images* for images of the coins.

3.2 Concentration of Metals

3.2.1 Initial Errors

XRF analysis yielded extensive information about the composition of the coins, as the raw data was conveniently supplied with attached concentration data. As will be later discussed, there were some issues with the normalisation of these data, though a normalised scale was devised (which includes values over 100).

Due to initial misdating, coin 4 was identified as a significant outlier due to its departure from trends. This resulted in the initial concentration to estimated typological date graphs appearing to have entirely non-uniform trends, as seen below.

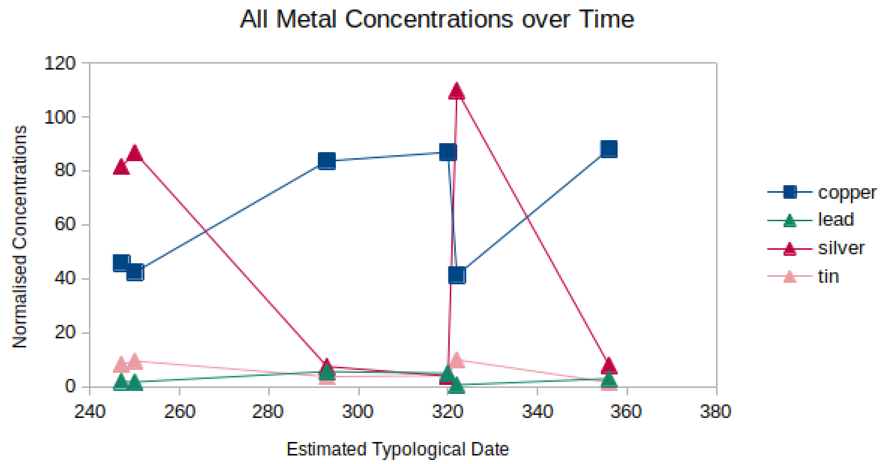

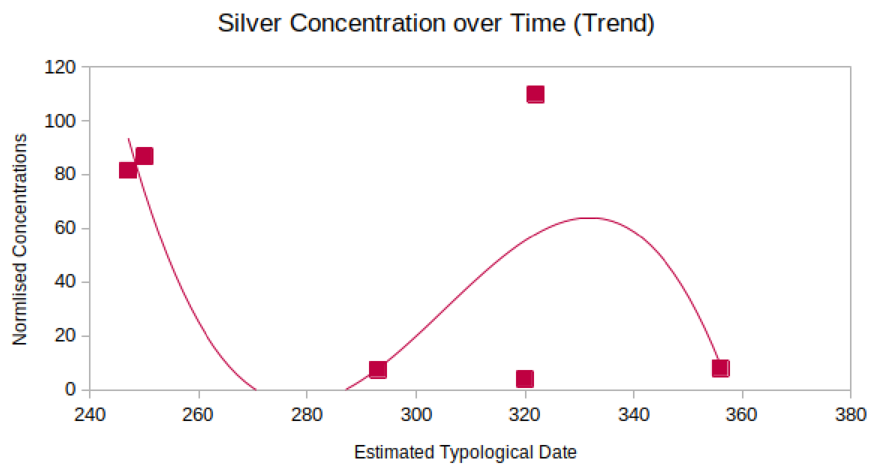

Having noted this outlier, I rechecked the typological placement of coin 4 and found it to be incorrect. After correction, the graphs appeared to be far more logical, showing logical trends that could be well fitted with a third-degree polynomial. However, the errors regarding the second and third coins remained, resulting in distinctly incorrect trends for lead and tin, and an overly steep trend for silver.

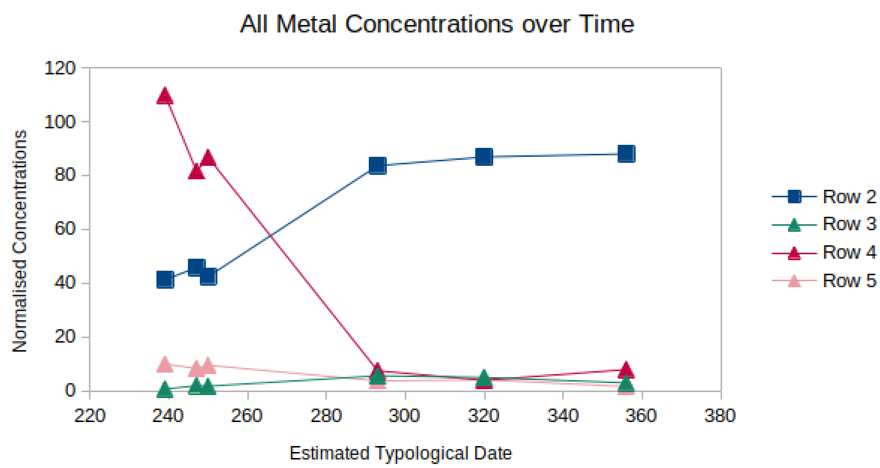

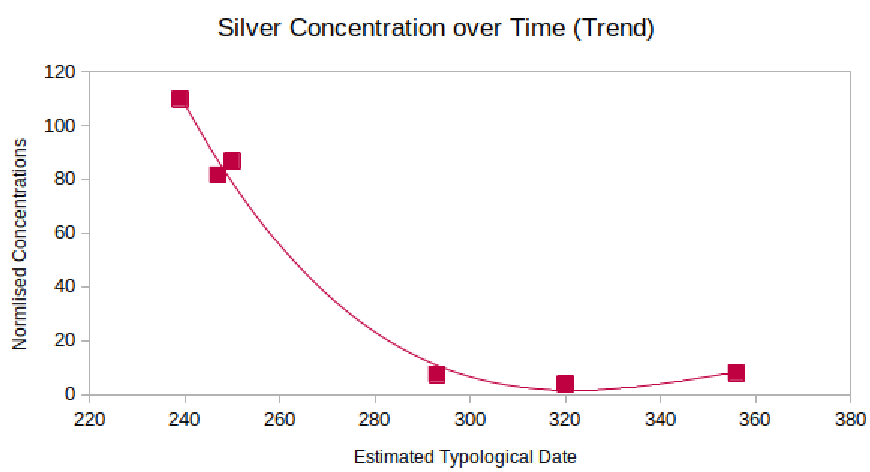

After the final correction of all known typological placement errors, all trend curves could be reasonably expressed with second-degree polynomials, except for silver, which is shown as a power to reflect the total decline in the currency's value. The alteration in the trends for lead and tin should also be noted from those which operated on

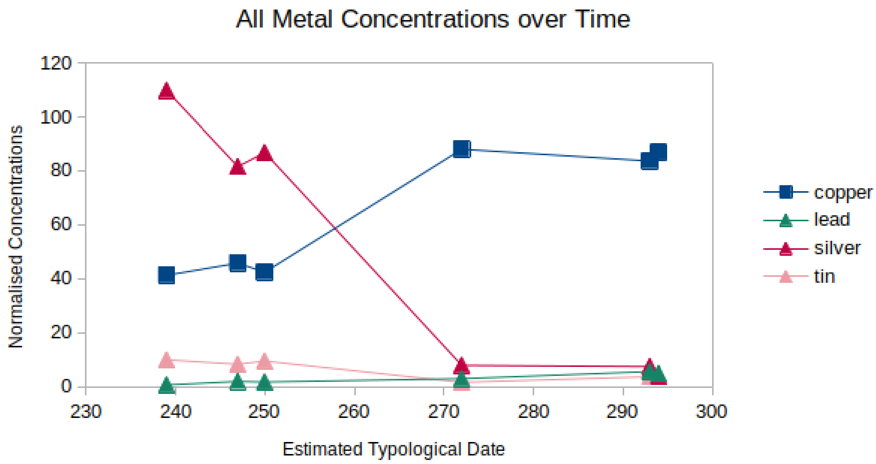

misdatings.

Having made these corrections, a number of useful observations can be made. All the final, corrected graphs are included in *Appendix 5 – Concentration Graphs*

3.2.2 Silver Concentration

The silver concentration declined significantly in these samples across time, decreasing from 109.75 in coin 4 (239 AD) to 3.97 in coin 2 (294 AD). This shows the debasement

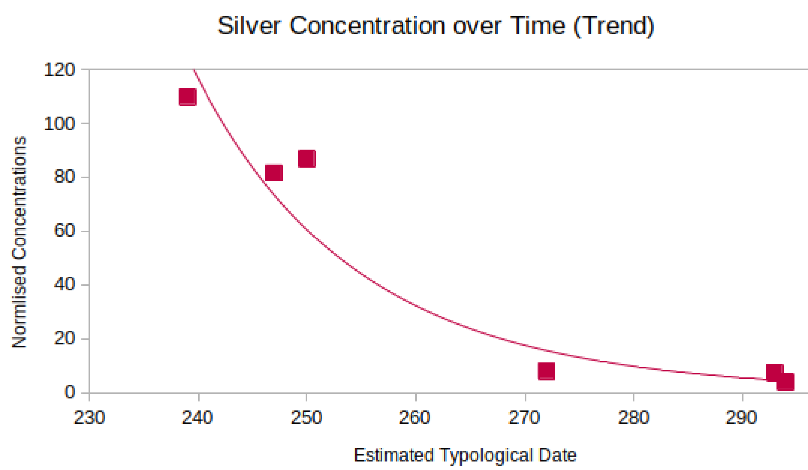

of the *antoninianus* and the extent thereof.

3.2.3 Copper and Tin Concentration

The copper concentration increased dramatically in these samples across time, from 41.31 in coin 4 (239 AD) to 87.98 in coin 3 (272 AD). After that date, the concentration drops to 83.61 in coin 1 (293 AD) and then recovers to 86.86 in coin 2 (294 AD).

The tin concentration decreased over time generally, though had an uptick distinctly to 3.75 and 4.14 in coins 1 and 2 (293 and 294 AD respectively) after a lower value of 1.64 in coin 3 (272 AD). However, as these metals were likely used together as bronze alloy (Pense 1992), they should be plotted together, as shown below. When this is done, we can see an almost perfect increase over time, from 51.28 in coin 4 (239 AD) to 90.997 in coin 2 (294 AD). This shows clearly that copper and tin were the primary metals used to replace silver under the debasement policies of the third century AD.

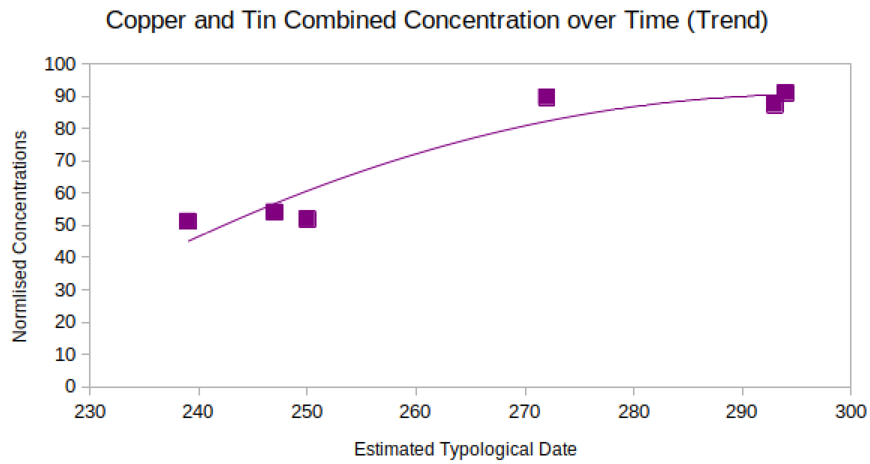

3.2.4 Lead Concentration

The lead concentration in this sample is interesting, as it appears to definitely increase over time, small as it is, making a relatively uniform progression from 0.70 in coin 4 (239 AD) to 5.02 in coin 2 (294 AD), peaking at 5.64 in coin 1 (293 AD). Without further data, it is difficult to identify the cause of this, though it can be said that the concentration of lead in these coins increases over time as they are debased.

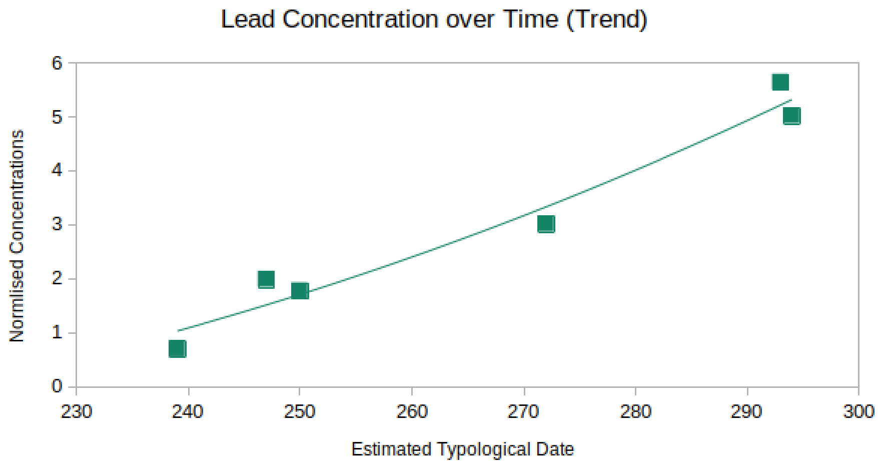

3.2.5 All Non-Silver Metals

If copper, tin, and lead are all combined into one major non-silver concentration graph, we can see clearly the trend of debasement as the silver concentration is rapidly replaced with these other metals. A quadratic trend curve fits excellently, to the point where it could even be made linear, as shown below.

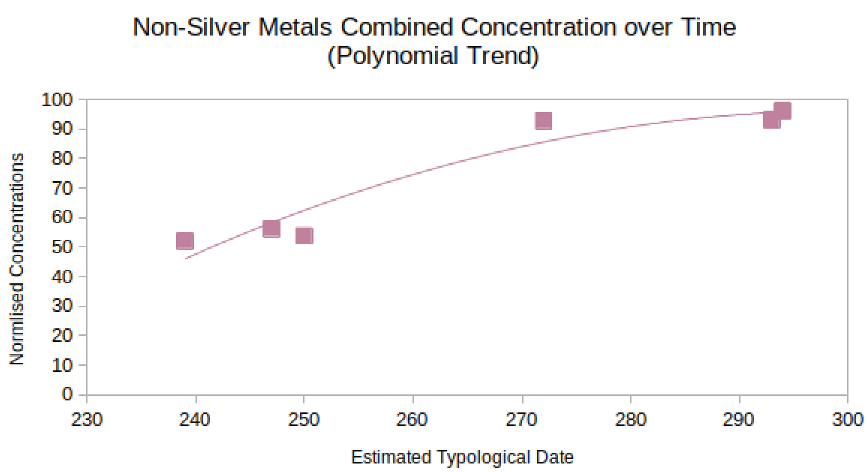

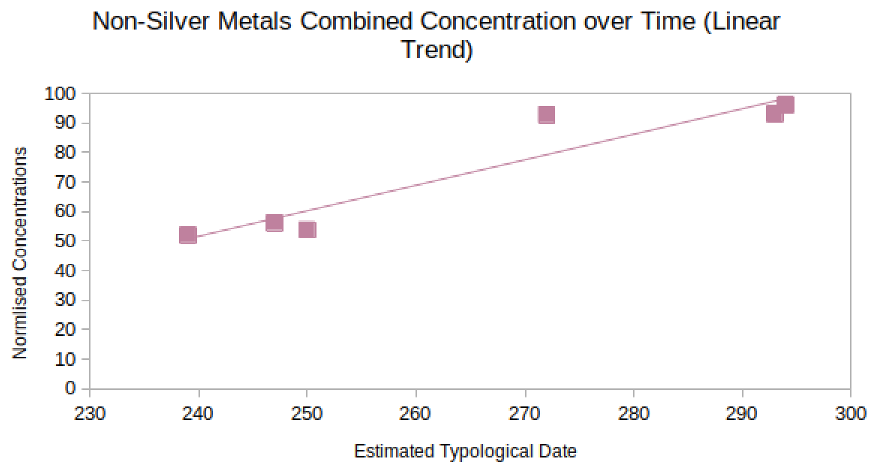

3.3 Raman Spectrometry

Raman analysis was done on the coins previously (pre-correction) thought to be the oldest and youngest, coins 5 and 3 respectively. It was hoped that this may lead to the identification of some information about the coins beyond the compositional data yielded by XRF, though this hope was misplaced. The four Raman spectra (scans were done of each side of the two coins) revealed almost no information whatsoever, except for the presence of carbon nitrogen bonds[1], which appear to indicate that the coins had been handled at some point, which is hardly surprising.

It should be noted that the scan of coin 5's obverse side was particularly noisy, and it was extremely difficult to ascertain any information whatsoever therefrom. This was possibly due to the surface of that side of that particular coin being too heterogenous in its topology, though it may also be due to the spectrometer simply not being held steadily enough.

These results are understandable, as Raman spectrometry is most useful for detecting organic bonds, which would only occur on the surface of coins given their production in high-heat environments.

See *Appendix 3 – Raman Spectra* for the full spectra, and *Appendix 6 – Raw Data* for the attempts to decode the peaks into identifiable bonds.

3.4 XRF Mapping

XRF mapping was performed on the obverse of coin 5 in a straight line across a flat part thereof. This data was found to be extremely difficult to process due to its large

[1] this analysis was performed using the online Raman peak identification assistance table at https://static.horiba.com/fileadmin/Horiba/Technology/Measurement_Techniques/Molecular_Spectroscopy/Raman_Spectroscopy/Raman_Academy/Raman_Tutorial/Raman_bands.pdf

size and unwieldy 3D graphs, so any analysis taken therefrom may be inaccurate.

While concentration data was not derivable from these graphs, they did appear to correlate reasonably well to the existing 'normal' XRF spectrum for the obverse of coin 5, and showed little differentiation overall. With further analysis, some additional data may be able to be derived from this, though the analysis of variations on a single coin was mostly beyond the scope of this project. Had it been possible to scan more than one face of one coin, a larger comparative analysis might have been possible.

3.5 Discussion

Beyond the more specific issues mentioned with the results, the following are a number of additional issues that impacted this project.

3.5.1 XRF Concentration Data

The concentration data presented were in a form such that they did not sum to 100, and large negative values were involved (e.g. -45 for NbKa1 of the reverse side of coin 6). Due to a lack of understanding about why this was the case, I simply took each concentration value and turned it into a percentage of the sum, meaning everything summed to 100. Negative values were then ignored, as none of the four major metals had them present. Some values though were above 100 (to account for the negatives), such as some of the copper concentrations. As a result, some inaccuracy may have been introduced into the analytical process through the ignoring of these negative values.

It should also be noted that scans were taken of both the obverse and reverse sides. These were turned into percentages and then averaged to form concentration data for each coin overall. This may also have adversely impacted accuracy, though as the two readings were each from the same coin, the effect should be minimal, provided there was not major variation between the two sides of any of the coins.

3.5.2 Dataset Size

Due to the small number of coins able to be analysed, and the lack of time for repetitions, analysis to control for the variable of time was unsuccessful (and is not included in this report). With a larger dataset, baseline concentration values of each metal may have been able to be arrived at for each mint, enabling the comparison of different metals across geography (e.g. which mints used more lead?). This analysis, while attempted, resulted in a dataset more strongly, and inversely, correlated to time, and as thus totally unsuccessful. It is nonetheless linked to in *Appendix 6 – Raw Data*.

3.5.3 Lack of Repetitions

Unfortunately, due to time and expense constraints, I was unable to perform more than one scan of each side of each coin, resulting in a total of only 12 XRF scans. With only one repetition of each, all data analysis is inherently unreliable, though it does appear to match with existing evidence (Pense 1992), and thus this does not appear to have affected accuracy to a major extent.

If this analysis were to be performed again, more scans should be taken if possible and averaged to arrive at more reliable data.

4 Conclusion and Further Direction

4.1 Conclusion

Having performed XRF spectrometric analysis in particular, it can be concluded that there is a distinct correlation between estimated typological date and the concentration of silver and non-silver metals. While trend curves show that a correlation can be drawn for each metal individually, due to the practical inseparability of these metals from alloys, such as bronze, which were likely used in Roman coin production (Pense 1992), they ought to be all taken together as major non-silver metals, in which case a correlation to date is clear.

With regards to these specific coins, they are from the mints Cyzicus, Antioch, and Roma, and all fall between 239-294 AD (see *Typological Placement* for all details). It should also be noted that coins 4-6, which appeared more silvery, did indeed have higher silver concentrations than the other three coins, and were older, further illustrating the aforementioned correlation.

As for the efficacy of Raman spectrometry on coins, the method proved almost totally useless, showing only really that the coins had been handled at some stage. Further, XRF mapping unfortunately proved to be of little relevance to this project due its specificity on a single coin.

4.2 Implications for Archaeology

This project has clearly shown the debasement of the Roman *antoninianus* in these samples and the replacement of silver with primarily copper. It has also shed light on the concentrations of lead and tin in these coins and has further demonstrated the efficacy of XRF spectrometry in the analysis of such third century AD Roman coins.

Further, this project has demonstrated the particular trends for each metal's concentration across the third century as the currency was debased, opening the door for a similar analysis on larger datasets and the arrival at a predictive model of concentration data from typological date.

4.3 Further Direction

This project has successfully typologically placed these coins and shown their concentrations, though a full predictive model of concentration from estimated typological date has not yet been attempted, and this would be a fascinating project that would allow the arrival at estimations of such data without the need for actual spectrometers to be used on every coin. While quadratic trends have been shown in this project, a far larger dataset would be needed to train a reasonable regression model.

Additionally, with a larger dataset, the variable of time could be attempted to be controlled (as was unsuccessful in this project), allowing the comparison of baseline metal concentrations between mints, which may reveal more about Roman trade routes by an analysis of the baseline concentrations of impurities in major metals used.

Finally, with a larger dataset of XRF mapping scans, variations in the concentrations of various metals across the surfaces of different coins could be compared, allowing far more nuanced and particular analysis which could shed greater light on the manufacturing process of such coins.

5 Reference List

Desjardins, Jeff. 2016. "Currency and the Collapse of the Roman Empire." *Visual Capitalist*. https://www.visualcapitalist.com/currency-and-the-collapse-of-the-roman-empire/.

"Gallienus Roman Emperor." n.d. *Encyclopedia Britannica*. Accessed June 11, 2021. https://www.britannica.com/biography/Gallienus.

Gentile, Claudio. n.d. "A Comparative Analysis of Old and Recent Ag Coins by XRF Methodology." Accessed April 9, 2021. https://www.academia.edu/4252404/A_comparative_analysis_of_old_and_recent_Ag_coins_by_XRF_methodology.

Metcalf, William E. 2012. *The Oxford Handbook of Greek and Roman Coinage*. Oxford University Press.

Pense, Alan W. 1992. "The Decline and Fall of the Roman Denarius." *Materials Characterization* 29 (2): 213–22. https://doi.org/10.1016/1044-5803(92)90116-Y.

6 Appendix

6.1 Appendix 1 – Coin Images

The following are the images of the coins studied. Please ntoe that they have been manually edited to remove the background, so if you happen to be studying the edges, *Appendix 6 – Raw Data* may be of more use to you.

Coin 1:

Coin 2:

Coin 3:

Coin 4:

Coin 5:

Coin 6:

6.2 Appendix 2 – XRF Spectra

The following are the XRF spectra for all six scans taken. Please note the differing scales for each spectrum in any comparison made. See *Appendix 6 – Raw Data* for more directly comparable data.

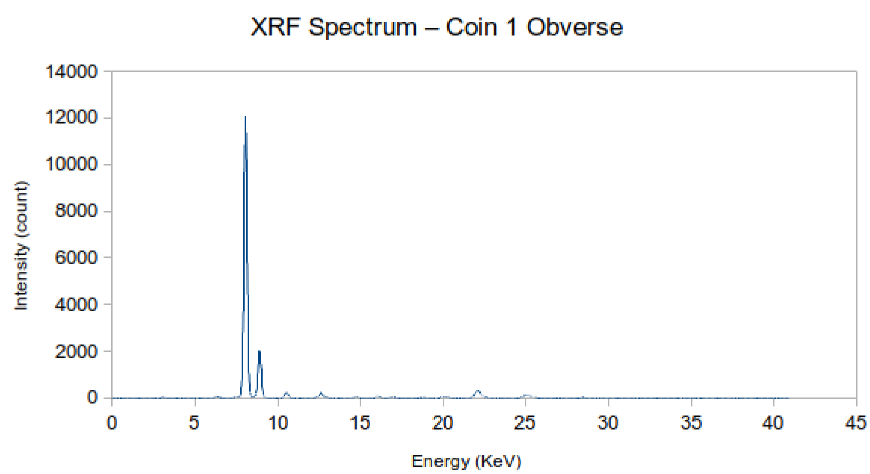

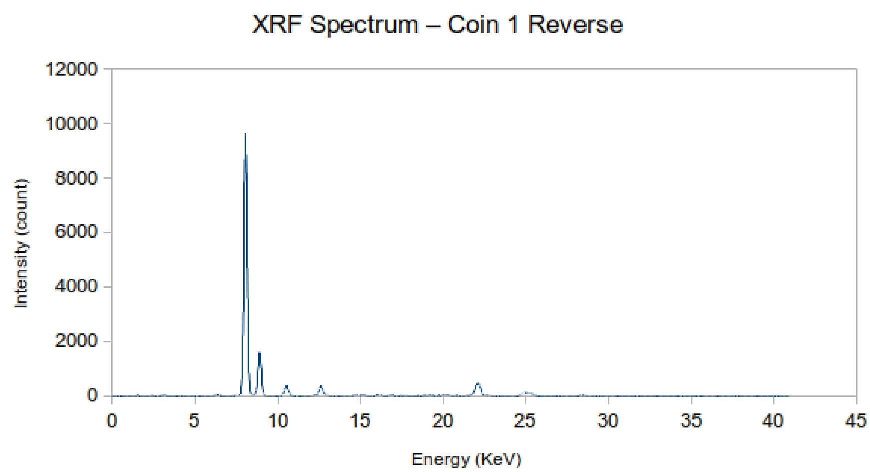
XRF Spectrum – Coin 1 Reverse
Intensity (count)
12000
10000
8000
6000
4000
2000
0
0
5
10
15
20
25
30
35
40
45
Energy (KeV)

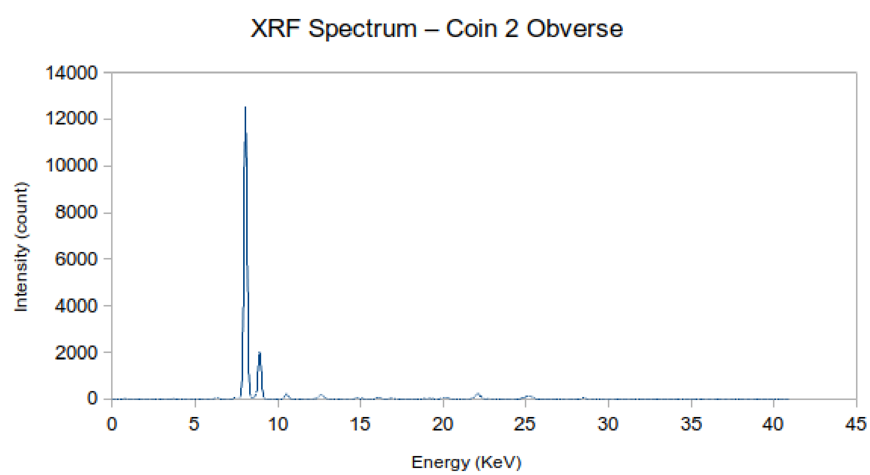
XRF Spectrum – Coin 2 Obverse
Intensity (count)
14000
12000
10000
8000
6000
4000
2000
0
0
5
10
15
20
25
30
35
40
45
Energy (KeV)

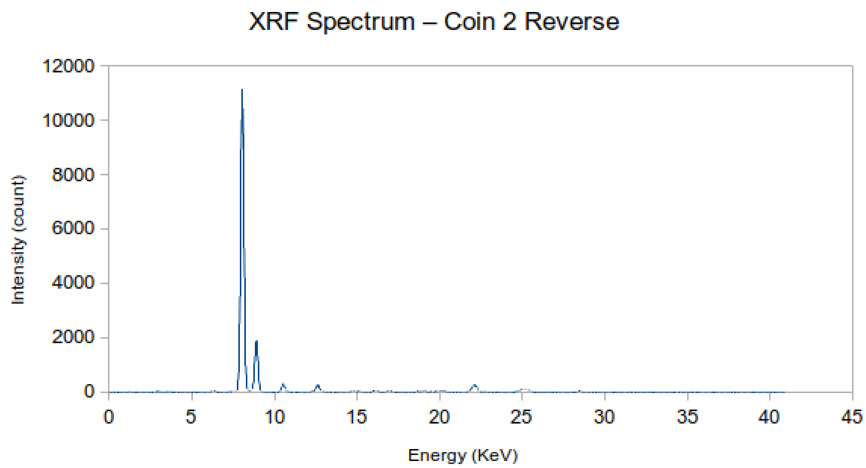
XRF Spectrum – Coin 2 Reverse
12000
10000
8000
6000
4000
2000
0
Intensity (count)
0
5
10
15
20
25
30
35
40
45
Energy (KeV)

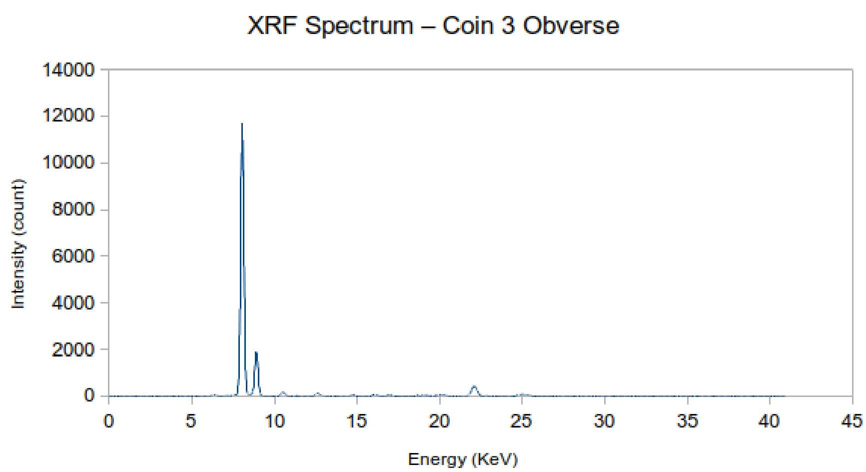
XRF Spectrum – Coin 3 Obverse
14000
12000
10000
8000
6000
4000
2000
0
Intensity (count)
0
5
10
15
20
25
30
35
40
45
Energy (KeV)

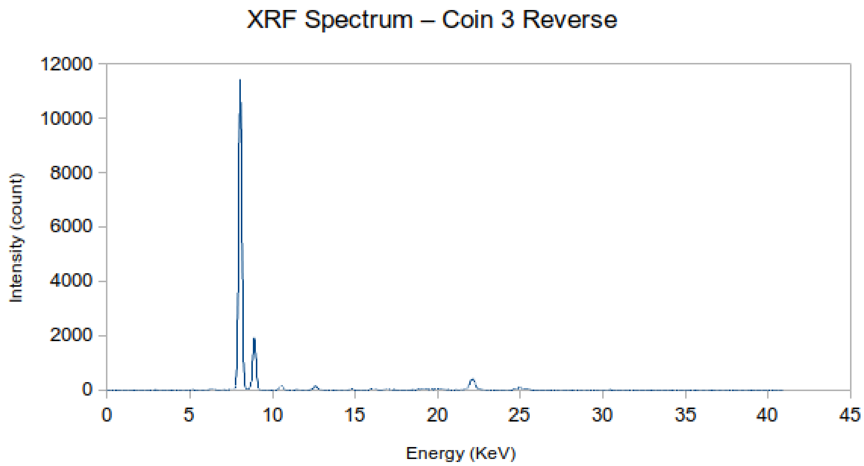
XRF Spectrum – Coin 3 Reverse
Intensity (count)
Energy (KeV)
12000
10000
8000
6000
4000
2000
0
0
5
10
15
20
25
30
35
40
45

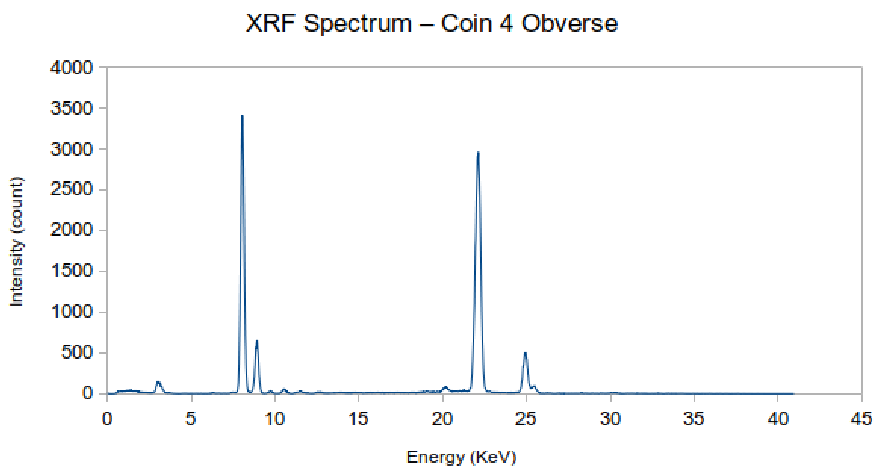
XRF Spectrum – Coin 4 Obverse
Intensity (count)
Energy (KeV)
4000
3500
3000
2500
2000
1500
1000
500
0
0
5
10
15
20
25
30
35
40
45

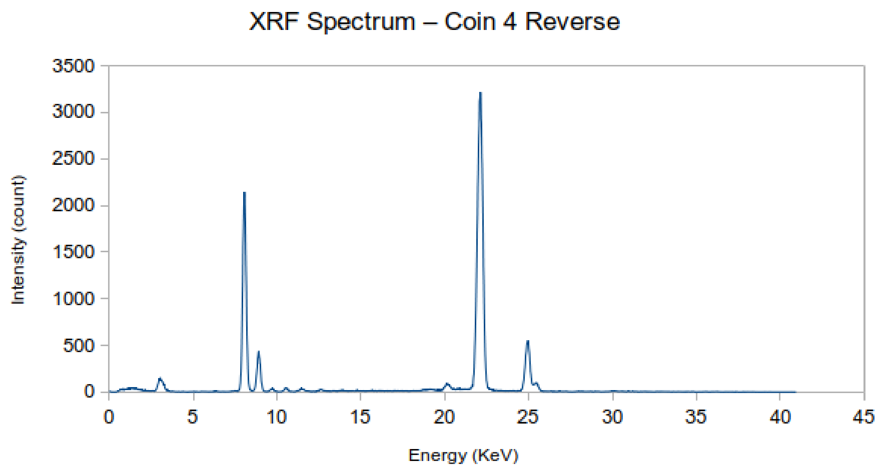
XRF Spectrum – Coin 4 Reverse
Intensity (count)
3500
3000
2500
2000
1500
1000
500
0
0
5
10
15
20
25
30
35
40
45
Energy (KeV)

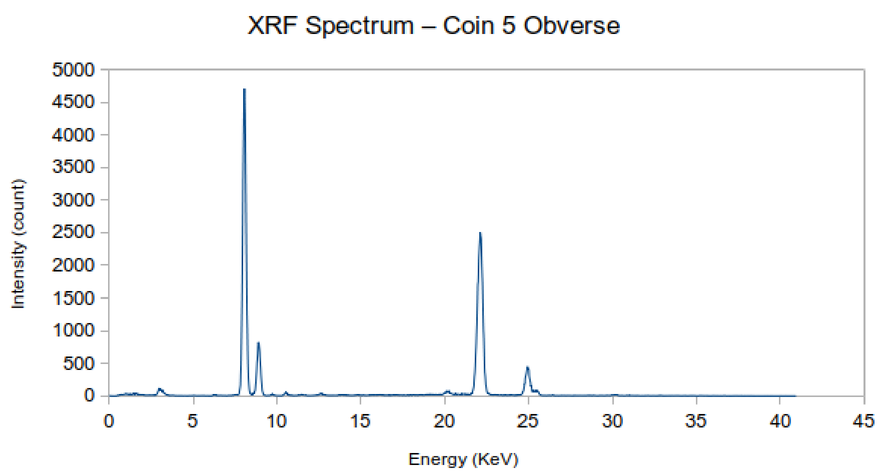
XRF Spectrum – Coin 5 Obverse
Intensity (count)
5000
4500
4000
3500
3000
2500
2000
1500
1000
500
0
0
5
10
15
20
25
30
35
40
45
Energy (KeV)

XRF Spectrum – Coin 5 Reverse

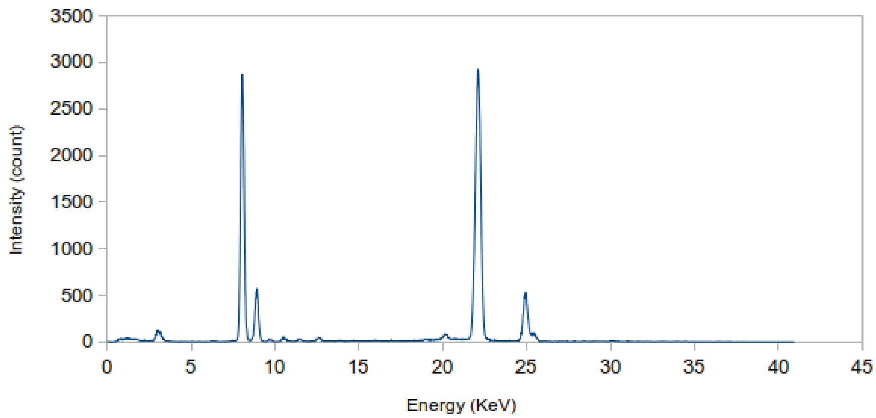

XRF Spectrum – Coin 6 Obverse

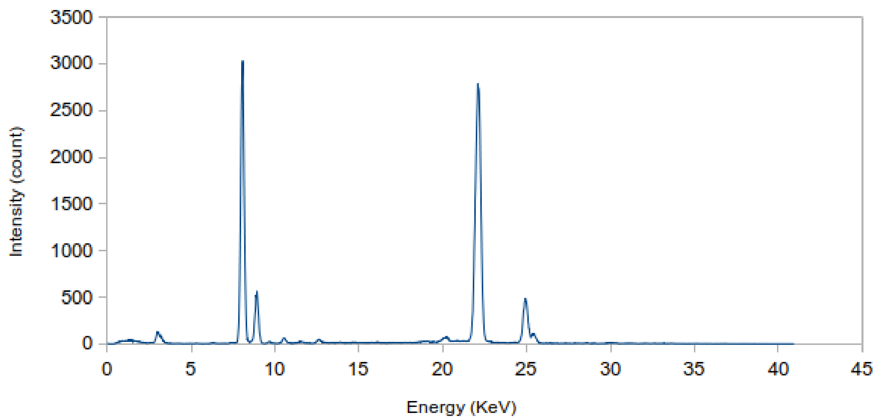

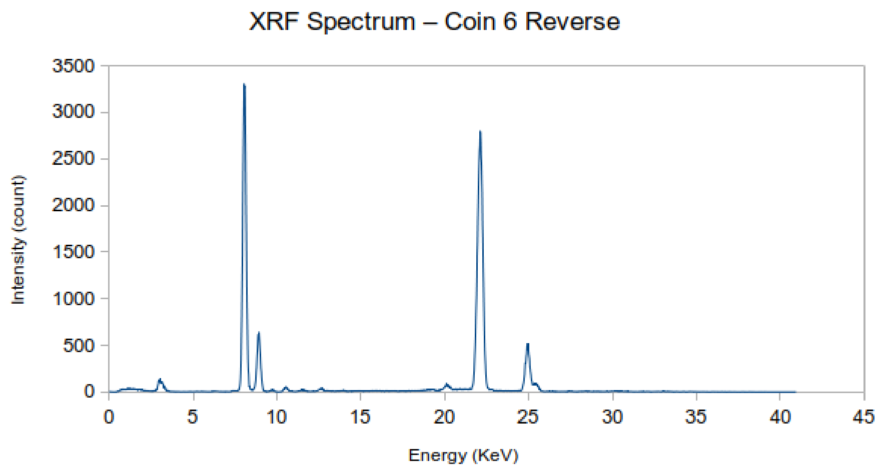

6.3 Appendix 3 – Raman Spectra

The following are the Raman spectra for both sides of the two coins scanned. These were originally thought to be the oldest (coin 5) and youngest (coin 3), though this was proven incorrect after corrections.

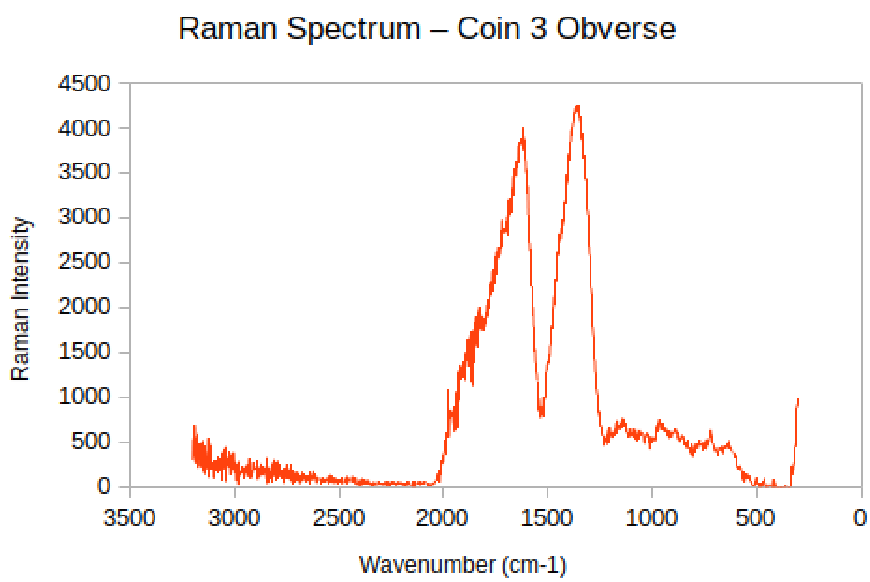

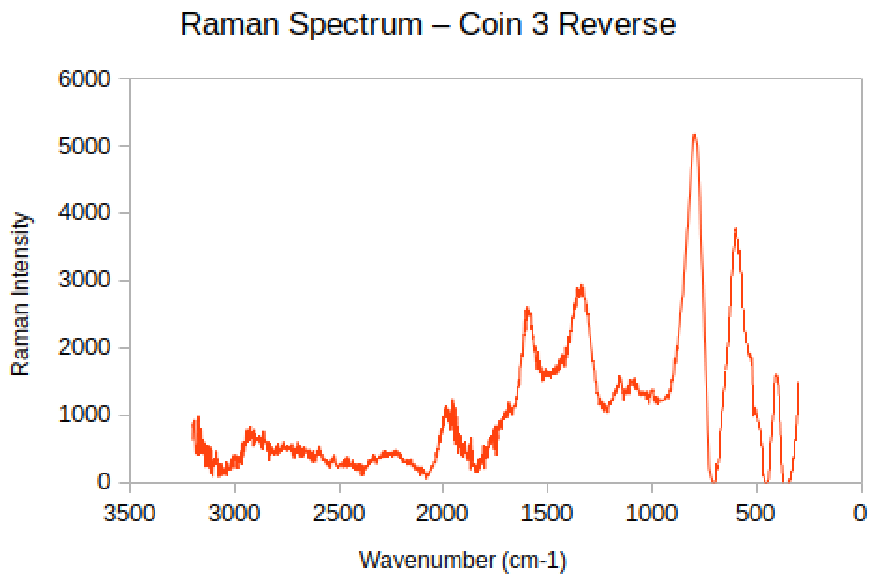
Raman Spectrum – Coin 3 Reverse
Raman Intensity
6000
5000
4000
3000
2000
1000
0
3500
3000
2500
2000
1500
1000
500
0
Wavenumber (cm-1)

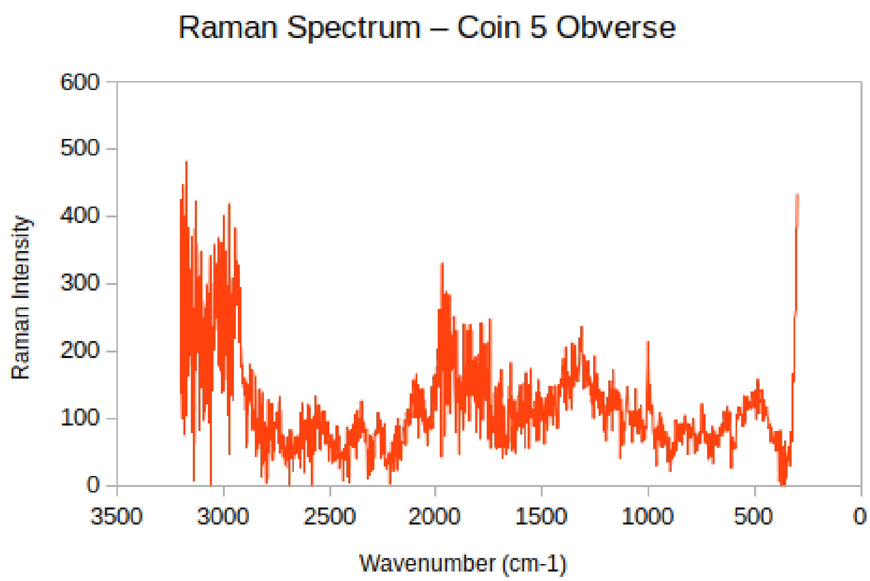
Raman Spectrum – Coin 5 Obverse
Raman Intensity
600
500
400
300
200
100
0
3500
3000
2500
2000
1500
1000
500
0
Wavenumber (cm-1)

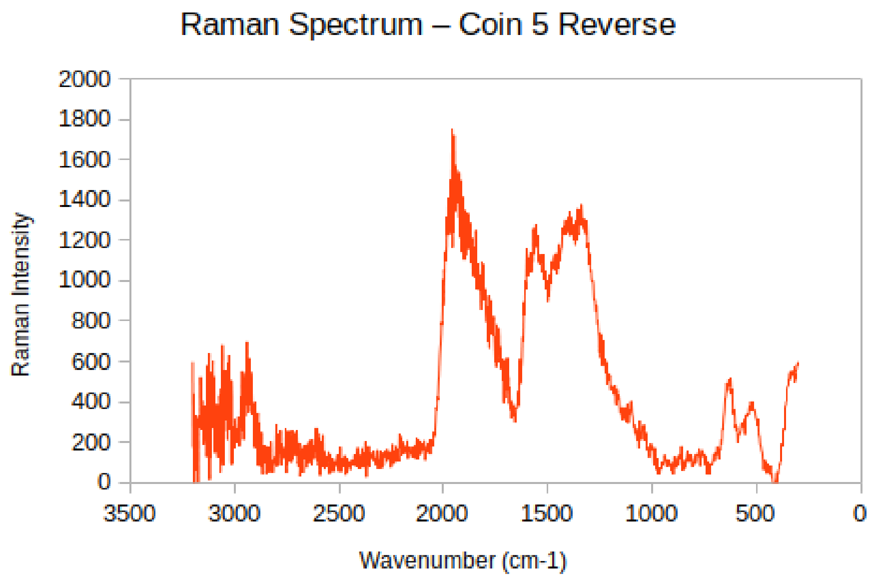

6.4 Appendix 4 – XRF Mapping Data

The following is a still image of the 3D XRF mapping spectrum for the obverse side of coin 5. The full `.fig` file (proprietary file format from MATLAB) can be opened with MATLAB for viewing and analysis, and is linked to in *Appendix 6 – Raw Data*.

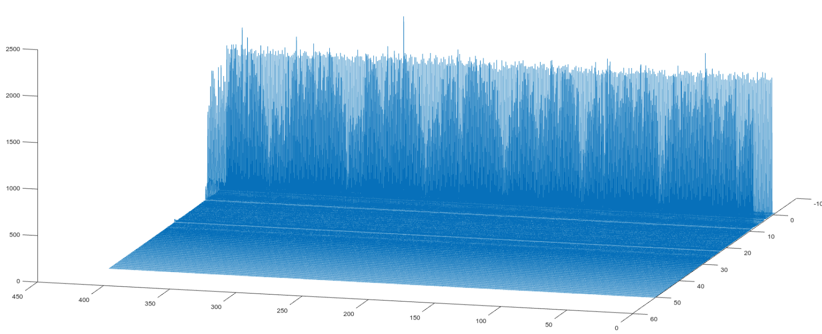

6.5 Appendix 5 – Concentration Graphs

The following are the graphs for the concentration of each major metal over estimated typological date. They represent the final iteration of analysis, after the correction of the three errors. With the exception of the first graph, all show trends. The graphs for copper, lead, and tin use second degree polynomial trend curves, while that for silver uses a power trend curve.

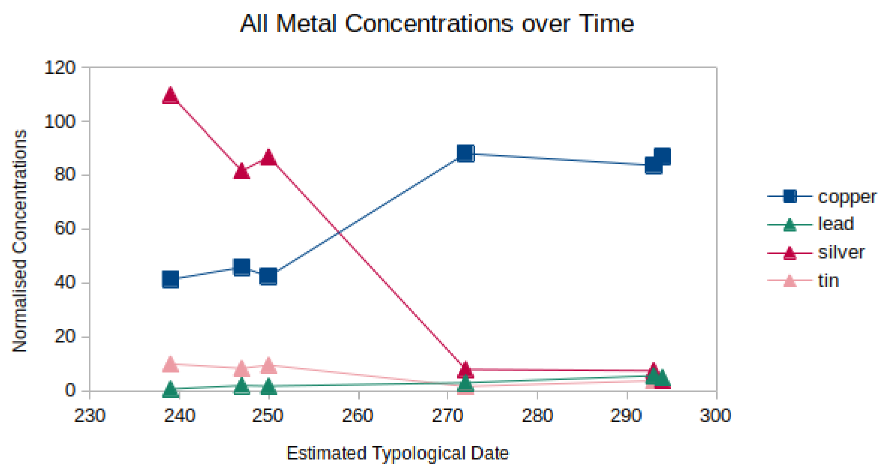

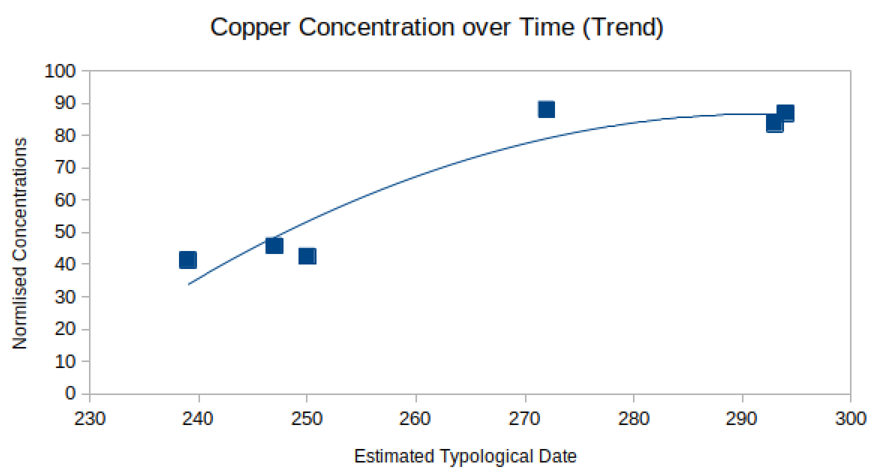

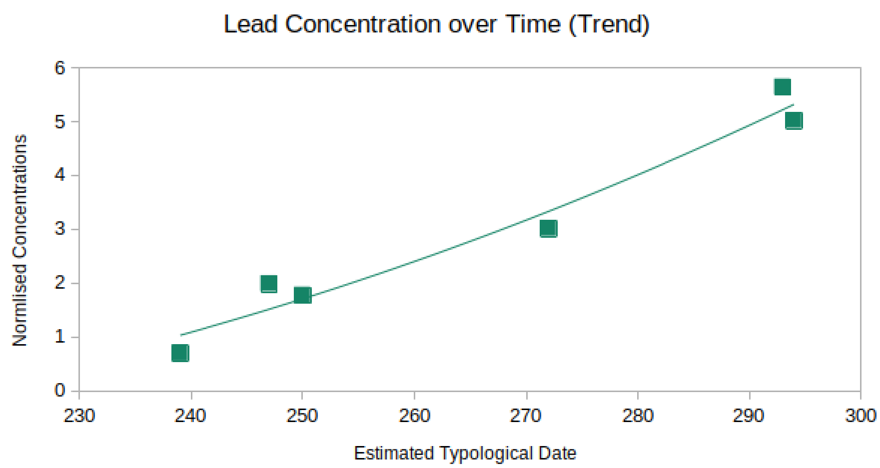
Lead Concentration over Time (Trend)
Normlised Concentrations
0
1
2
3
4
5
6
230
240
250
260
270
280
290
300
Estimated Typological Date

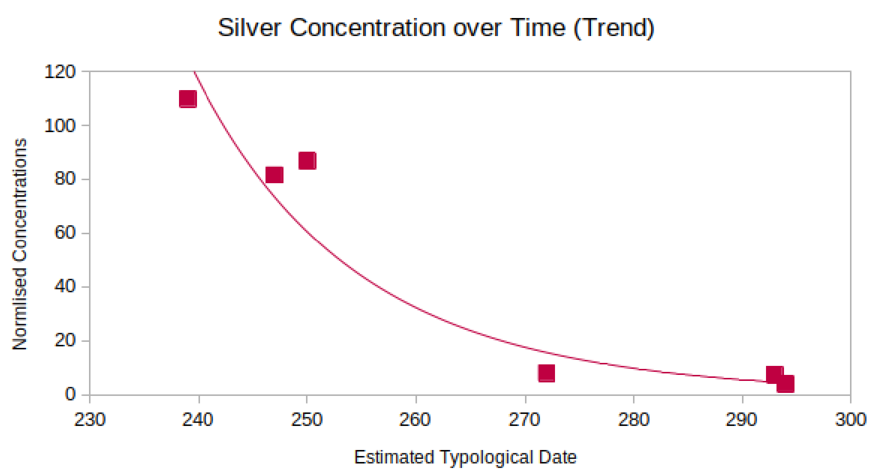
Silver Concentration over Time (Trend)
Normlised Concentrations
0
20
40
60
80
100
120
230
240
250
260
270
280
290
300
Estimated Typological Date

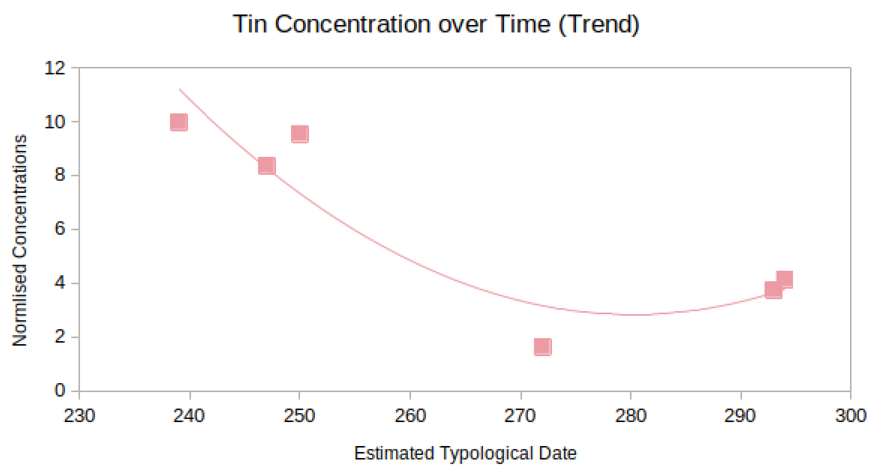

Tin Concentration over Time (Trend)
Normlised Concentrations
Estimated Typological Date
0
2
4
6
8
10
12
230
240
250
260
270
280
290
300

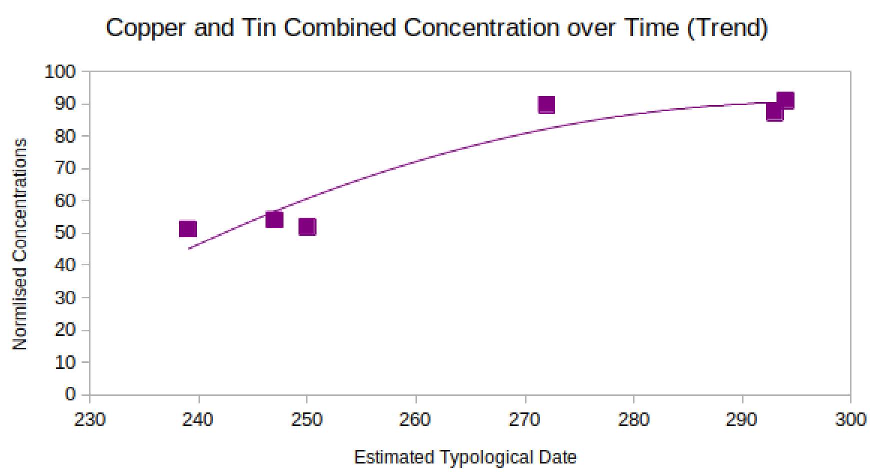

Copper and Tin Combined Concentration over Time (Trend)
Normlised Concentrations
Estimated Typological Date
0
10
20
30
40
50
60
70
80
90
100
230
240
250
260
270
280
290
300

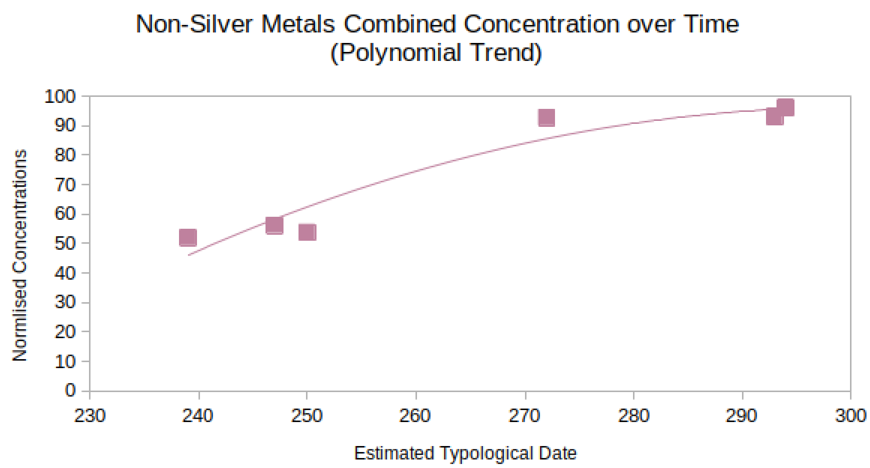

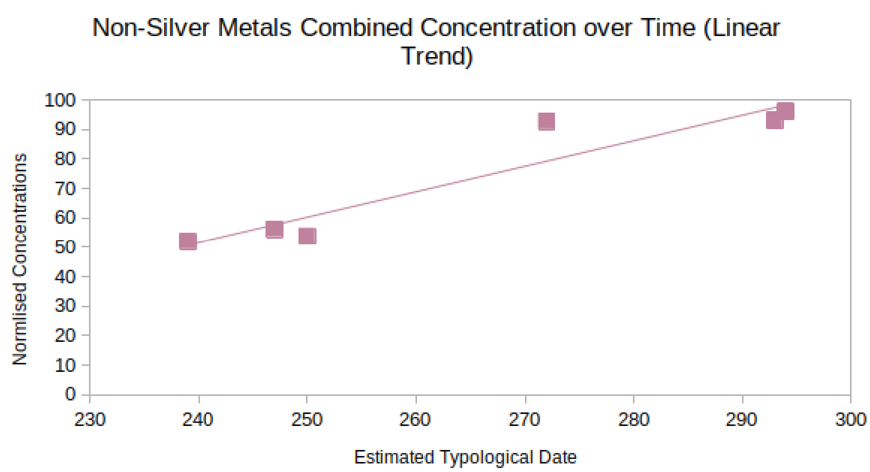

6.6 Appendix 6 – Raw Data

TODO GH links to all graphs